Engineering Geology 297 (2022) 106509

Contents lists available at ScienceDirect

Engineering Geology

journal homepage: www.elsevier.com/locate/enggeo

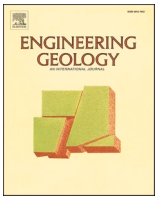

Assessing the influence of the hydraulic boundary conditions on clay slope stability: The Fontana Monte case study

Annamaria di Lernia [a,*], Federica Cotecchia [a], Gaetano Elia [a], Vito Tagarelli [a], Francesca Santaloia [b], Giuseppe Palladino [c]

[a] Department of Civil, Environmental, Land, Building Engineering and Chemistry (DICATECh), Technical University of Bari, via Orabona 4, 70125 Bari, Italy
[b] IRPI, National Research Council, Bari, Italy
[c] Department of Geology and Geophysics, School of Geosciences, University of Aberdeen, Aberdeen, UK

ARTICLE INFO

Keywords:
Weather-induced landslide
Slope-vegetation-atmosphere interaction
Uncoupled hydraulic approach
Numerical modelling

ABSTRACT

Recent studies have assessed that slope-vegetation-atmosphere, SLVA, interaction may trigger the activity of deep landslides in clayey slopes. In some cases, the presence of an underground aquifer, fed by an upstream hydraulic recharging area, may represent a predisposing factor of such activity, being co-responsible of deep piezometric heads, which can undergo seasonal fluctuations due to the SLVA interaction. In this perspective, the present paper illustrates the results of a scientific research, carried out in a pilot site of the Daunia Apennines, the Fontana Monte slope at Volturino (Foggia, Italy), considered as a prototype of the class of landslide mechanisms controlled by both the rainfall water infiltration and the presence of a water-bearing aquifer in the hillslope.

Numerical simulations of the saturated/partially saturated transient seepage flow in the slope have been performed by means of uncoupled hydraulic finite element analyses, with the aim of investigating the sources of large piezometric heads, related to climatic, hydrogeological and hydraulic slope features. The rainfall and evapotranspiration fluxes, the latter defined through the FAO Penman-Monteith method, are both implemented as ground surface input, while seasonal variations of the upstream hydraulic boundary conditions are imposed to predict the seasonal piezometric excursion at shallow and deep monitoring points. The transient seepage results are then used as input for limit equilibrium analyses to assess the influence of the hydraulic settings on the stability of the considered landslide body. The work shows the impact of both climatic and hydraulic factors on the seepage processes, affecting the stability of the slope. Moreover, it is highlighted that the accurate implementation of the upstream hydraulic feeding is fundamental for a reliable prediction of the monitored piezometric regime, strictly related to the recharge of the water-bearing aquifer.

1. Introduction

It is well-recognised that the equilibrium conditions in slopes may be affected by the interaction of the soils with the atmosphere, which determines the variation of the pore water pressures with time, in turn affecting the stress-strain behaviour and the overall stability of the slope (Cascini et al., 2010a; Elia et al., 2017; Rouainia et al., 2020; Sitarenios et al., 2021; Smethurst et al., 2012; Tsiampousi et al., 2017; Vassallo et al., 2015). Recent scientific literature has highlighted the influence of climatic factors on landslide activity, not only for slopes formed of permeable materials (Ng and Shi, 1998; Pirone et al., 2012; Rahardjo et al., 2009), or clayey slope covers of less than 10 m thickness (Kenney and Lau, 1984; Vaughan, 1994), but also for slopes made of clays and location of deep landslides (Alonso et al., 2003; Cotecchia et al., 2019a, 2016b, 2015, 2014; Leroueil, 2001; Pedone et al., 2018; Tommasi et al., 2013). Indeed, the climatic factors, such as rainfall, temperature, net solar radiation, wind and relative humidity, together with the vegetation and the soil properties are responsible for water exchange phenomena between the topsoil and the atmosphere. In particular, the amount of water infiltrating in the slope, defined 'net rainfall' in the following (Cotecchia et al., 2019a), depends on the rainfall intensity, the runoff, the water evaporation from the non-vegetated soil outcrop and the transpiration from the vegetation, and typically produces a variation in the pore water pressure distribution across the whole slope with time,

* Corresponding author.
E-mail addresses: annamaria.dilernia@poliba.it (A. di Lernia), federica.cotecchia@poliba.it (F. Cotecchia), gaetano.elia@poliba.it (G. Elia), vito.tagarelli@poliba.it (V. Tagarelli), f.santaloia@ba.cnr.irpi.it (F. Santaloia), giuseppe.palladino@abdn.ac.uk (G. Palladino).

https://doi.org/10.1016/j.enggeo.2021.106509
Received 1 June 2021; Received in revised form 30 October 2021; Accepted 22 December 2021
Available online 28 December 2021

which impacts the stability of the slope more or less significantly (Fredlund et al., 2012; Gens, 2010; Lu and Likos, 2004). The whole set of interaction phenomena between the slope soils, the climatic agents and the vegetation, controlling the cited water exchange fluxes and the corresponding slope equilibrium conditions, is generally referred to as "slope-vegetation-atmosphere (SLVA) interaction".

The extent to which the SLVA interaction is critical for the slope stability depends also on the internal factors of the slope (Terzaghi, 1950), e.g. on the mechanical and hydraulic constitutive behaviour of the slope soils, and on the hydraulic conditions along the underground slope boundaries. Furthermore, the latter may vary over time as effect of the response to climate of the whole hydrogeological basin within which the slope is located. Therefore, accounting for the variations over time of the underground hydraulic boundary conditions of the slope may be critical for a proper assessment of the SLVA interaction. For example, in slopes made of fine soils bearing rocky aquifers, the response to climate of the groundwater in the rocky aquifer may be responsible for part of the piezometric fluctuations in the fine soils, adding to the effects on the piezometric levels of the climatic action at the top boundary of the slope (Brönnimann et al., 2013; Cai and Ofterdinger, 2016; Greco et al., 2014; Healy and Cook, 2002; Lorenzo-Lacruz et al., 2017; Piccinini et al., 2014; Wang et al., 2019).

The effects of the SLVA interaction on the stability of slopes can be assessed through modelling strategies of different level of complexity, ranging from uncoupled hydraulic (H), to thermo-hydraulic (TH), to coupled hydro-mechanical (HM) (Elia et al., 2017). The H modelling simulates the transient seepage due to the water exchanges caused by rainfalls and evapotranspiration, disregarding both the energy balance and the momentum balance of the slope system (Calvello et al., 2008; Cascini et al., 2010a, 2010b; Cotecchia et al., 2019a, 2014; Tagarelli and Cotecchia, 2020b). Therefore, the water infiltration is estimated a priori and the slope stability is assessed via limit equilibrium (LE) analyses, employing as input the pore water pressures resulting from the H modelling (Cotecchia et al., 2019a; Ng and Shi, 1998; Van Esch et al., 2013). The HM approach can be adopted to assess the slope displacements resulting from the cyclic variation of the pore water pressures, through the coupled solution of the momentum-balance and mass-balance equations, still inputting the water infiltration flow estimated a priori (Elia et al., 2020; Kovacevic et al., 2001; Lollino et al., 2016; Pedone et al., 2021; Postill et al., 2021; Rouainia et al., 2020, 2009; Sitarenios et al., 2021; Tagarelli and Cotecchia, 2020a). The TH modelling, instead, allows for the prediction of both the pore fluid pressure and temperature variations, accounting for the energy balance equation and computing the water transition from the liquid to the vapour phase (Olivella et al., 1996, 1994; Rajeev et al., 2012). The most advanced numerical approach would account for the thermo-hydro-mechanical (THM) coupling of the processes occurring in the slope interacting with climate. However, the complexity of the mathematical formulation makes this approach still a challenge. In any case, irrespective of the adopted numerical strategy, the computation of the SLVA interaction effects requires the input in the model of several slope factors (Terzaghi, 1950), such as the slope lithostratigraphic and geo-structural set-up, the hydro-mechanical constitutive laws of the lithotypes and the climatic and hydrogeological boundary conditions. It follows that a reliable prediction of the SLVA interaction and of its effects on the slope stability requires a thorough investigation of such factors and a phenomenological interpretation of the slope processes, which may guide the design of the slope modelling.

According to these premises, a research study of the SLVA interaction effects for natural slopes located within a geologically complex region, i.e. the Eastern sector of the Southern Apennines over-thrusting the Foredeep deposits, has been carried out. Indeed, this region is characterised by the recurrency of landslide activity in late winter-early spring. With particular reference to clay slopes, an intense research into the factors and stability conditions has provided evidence of the recurrence of landslide activity in slopes location of clayey flysch and very high piezometric heads down to large depths (e.g. 50 m) (Cafaro et al., 2017; Cotecchia et al., 2020, 2019a, 2016c, 2014, 2010; Losacco et al., 2021; Pedone et al., 2021; Tagarelli and Cotecchia, 2020b). Often, the clayey soils involved in the landsliding are characterised by low strength parameters, due to both their high plasticity and fissuring. Therefore, the low soil strength parameters and the high piezometric heads represent predisposing factors of landsliding in these slopes. Besides, seasonal fluctuations of the pore water pressure have been recorded in the same slopes, plausibly representing an effect of the SLVA interaction. Such fluctuations have been recognised to trigger the reactivation of pre-existing landslide bodies in several cases, as exemplified in Fig. 1 for two representative case studies, the Pianello slope (Bovino, FG; Cotecchia et al., 2016c; Losacco et al., 2021; Palmisano et al., 2018) and the Pisciolo slope (Melfi, PZ; Cotecchia et al., 2014, 2019a; Pedone et al., 2018; Tagarelli and Cotecchia, 2020b, 2020a). The Pianello landslide is characterised by accelerations (see the inclinometric monitoring data in Fig. 1a) concurring with the rise of the piezometric heads occurring by the end of summer to early spring, in turn concurring with the rise of the 180-day cumulative rainfalls. Similarly, in the Pisciolo slope seasonal variations of the piezometric heads down to large depths (i.e. 60 m) have been shown to trigger the acceleration of deep landslide bodies (Fig. 1b). Therefore, the monitoring data and the timing of records of landslide damages on structures and infrastructures interacting with the landslide bodies have testified that deep displacement accelerations in clay slopes across the region are recurrently related to the SLVA interaction.

The Fontana Monte slope (Volturino, FG, Italy) is one of the several slopes that, in the geo-hydro-mechanical (GHM) context here of reference, is location of landslide activity on a seasonal timespan, as testified by field records of damages to buildings and roads located either about the rear scarp of the landslide body or above it and by deep displacement records (Cotecchia et al., 2011). As such, the Fontana Monte slope has been used as reference to carry out numerical analyses of the prototype SLVA interaction problem for the region, with the specific aim of investigating the influence of the hydraulic boundary conditions on the piezometric regime in the slope and, consequently, on its stability. The results of such research study are reported in the paper, in order to provide a further contribution to the interpretation of the SLVA interaction phenomena for clayey slopes, highlighting the extent to which they depend not only on the interaction with the climatic agents of the sloping top boundary, but also on the hydrogeological boundary condition and on its connection with the climatic variables.

2. The Fontana Monte case study

The Fontana Monte slope, located in the north-western hillslope of the Volturino urban centre, is location of a large slow-moving deep-seated landslide (see Figs. 2 and 3), involving mainly clays belonging to the Toppo Capuana (TPC) formation of medium to high plasticity and random to oriented fissuring of medium intensity (Vitone and Cotecchia, 2011). The analysis of historical data and topographic maps, from 1848 till 2000, have revealed the ancient nature of the Fontana Monte landslide, which was already active in the nineteenth century (Lollino et al., 2016, 2010). Currently, the slope activity is the result of the evolution of straining along pre-existing shear bands.

As for other slopes in the same GHM context of reference, the Fontana Monte slope is location of soils characterised by low strength parameters and high piezometric heads down to large depth. The large piezometric heads add to the weakness of soils as internal predisposing factor of the deep landslide activity (Lollino et al., 2016, 2010). Fig. 4a illustrates the piezometric head variations with time recorded by means of piezometers installed at 25.5 m and 49 m depth down the borehole SC1, at 4.4 m and 25 m along borehole SC2 and at 15.4 m along the borehole SC3 (see Figs. 2 and 3 for their locations). The monitoring data, from 2008 to 2013, are those reported in Lollino et al. (2010, 2016), while new data have been logged from 2015 to 2021. Although the monitoring data are not continuous with time, they clearly show that the

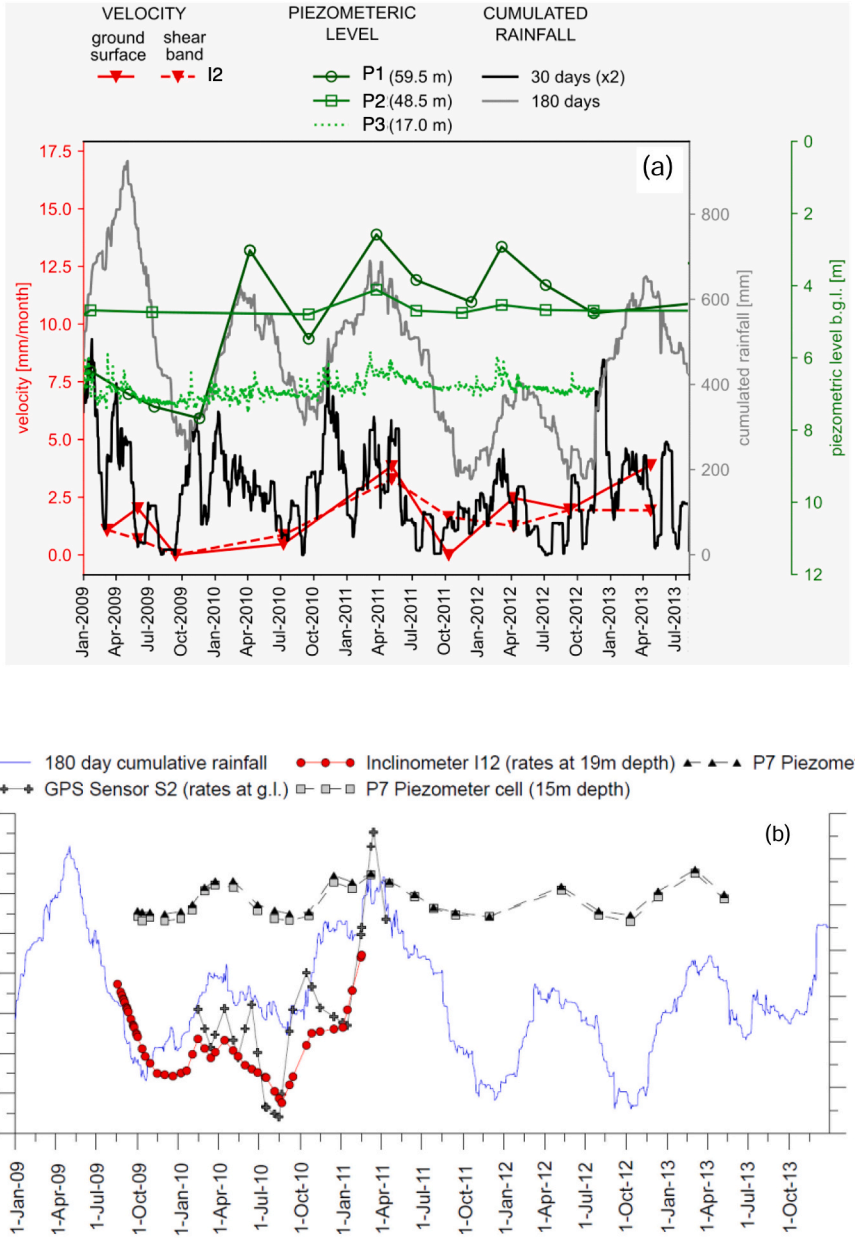

Fig. 1. Variation with time of the recorded rainfalls, 180-day cumulative rainfall and in-situ monitoring data (piezometric heads and displacement rates) for (a) the Bovino case study (Losacco et al., 2021) and (b) the Pisciolo case study (Tagarelli and Cotecchia, 2020a).

piezometric levels measured along both SC1 and SC3 boreholes are very high (between about 2 m b.g.l. in winter and 4 m b.g.l. in summer) even at large depths (i.e. 49 m b.g.l). Moreover, both the piezometers installed in borehole SC1, at 25.5 m and at 49 m depth, measured almost the same piezometric level, cyclically oscillating between a maximum value in winter and a minimum one in summer.

It is worth highlighting that the piezometric levels measured by means of the piezometers installed in borehole SC2 are out of trend with respect to the other data, due to the borehole location in the downslope area, where the soil profile is relatively more heterogeneous. Accordingly, the deeper piezometric cell in SC2 monitored piezometric levels ranging from 8 m to 10 m b.g.l., whereas the shallower cell, installed within a coarse soil layer, recorded levels between 3 m and 5.5 m above ground level.

As recurrent in the GHM context of reference, the Fontana Monte landslide suffers from seasonal reactivations, with the rate of movements increasing in winter and reducing during the dry season, as documented by inclinometric data and by the damages observed on buildings and roads close to the crest and along the borders of the landslide body. Fig. 4a illustrates the time variations in displacement rate logged at 24 m depth along the inclinometer SD1, at 45 m depth along the inclinometer SD2 and at 27 m depth along the inclinometer S1V, corresponding to the depths at which the active shear band has been identified. The average rate of movement is about 0.1–0.15 mm/month during the dry season and may reach 0.25–0.3 mm/month in winter. The overall seasonal trend of the slope movements is more evident in the period between September 2008 and September 2010 (Fig. 4b), for which more monitoring data are available and provide a better evidence of the fluctuations of the piezometric heads (between a maximum value at the end of the winter-early spring and a minimum value at the end of the summer), in accordance with the seasonal variation of the 180-day cumulative rainfalls and a concurring variation of slope movement rates (Lollino et al., 2016, 2010). Hence, the general trend of such seasonal excursions resembles that typically observed in

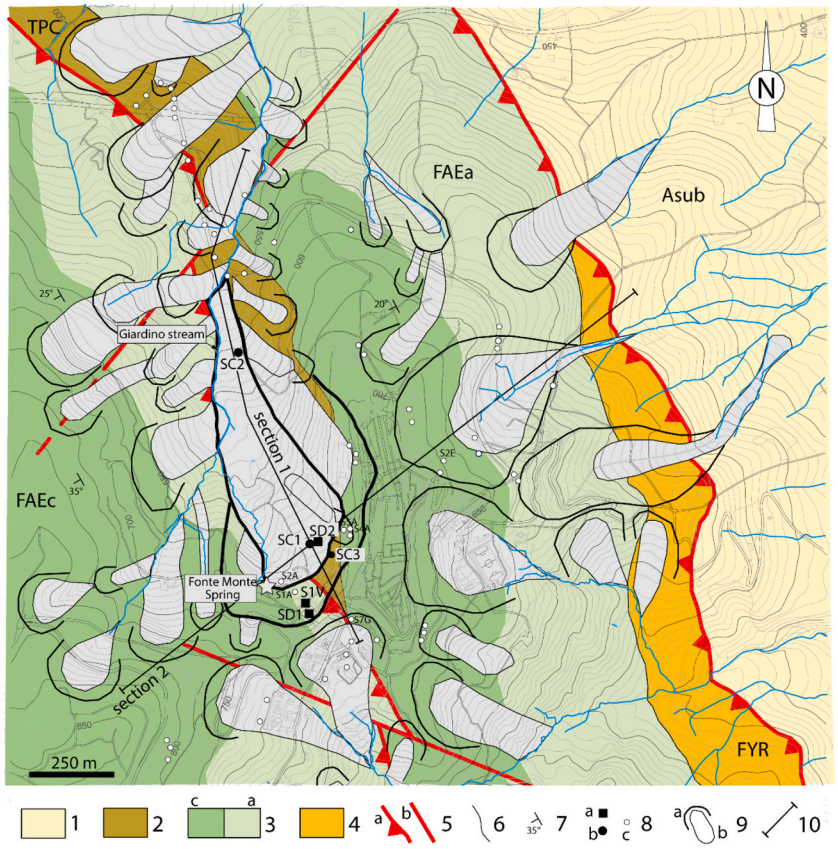

Fig. 2. Geological map of the Volturino area. Legend: 1. Asub; 2. TPC; 3. Limestone member (FAEc) (c) and clayey member (FAEa) (a) of Faeto Flysch; 4. FYR; 5. Overthrust (a) and fault (b; dashed if inferred); 6. stratigraphic contact; 7. Bedding (dip in degree); 8. boreholes hosting inclinometer (a) or piezometer (b) drilled during the 2008–2012 campaigns; (c) previous field investigations; 9. Landslide (a-crown, b-body); 10. section traces.

the slopes of the same GHM context of reference (Fig. 1) and the Fontana Monte landslide activity is believed to be connected to the seasonal excursions of pore water pressures at large depths (i.e. even at about 50 m b.g.l), and their connection with the SLVA interaction impacts on the operational strengths along the deep ancient slip surface in the slope (Cotecchia et al., 2016a; Lollino et al., 2016, 2010).

According to such phenomenological interpretation, the Fontana Monte slope has been deemed to be appropriate as a prototype slope, to carry out a numerical computation of the effects of the SLVA interaction on the stability of slopes in the GHM context of reference. According to these data, the slope is location of a thick clay stratum bearing a calcareous bedrock hosting an aquifer, which is fed at the top of the slope, where the calcareous rock outcrops, as shown in the sections in Fig. 3. The direct contact of the low permeability clay and the far more permeable rock represents an important underground boundary condition of the slope, which is much neater in the Fontana Monte slope than in other case studies. Therefore, this slope has been considered particularly suitable for the investigation of the influence of the underground boundaries on the slope hydraulics and stability through numerical modelling. In particular, this paper discusses the impact on a prototype clay slope, of the GHM context of reference, of the regime of the deep rocky aquifer combined with climatic action at the ground surface.

With reference to the Fontana Monte slope, Lollino et al. (2016, 2010) carried out finite element H and coupled HM analyses, in which the variations in piezometric head from summer to winter were computed through the simulation of a steady-state summer-like seepage at first and a winter-like seepage afterwards. Such numerical modelling already proved the tendency of deformations in the slope to reactivate in the late winter, when the piezometric heads are highest, as typically observed in the GHM context of reference (Cafaro et al., 2017; Cotecchia et al., 2019b, 2010). The numerical modelling illustrated in the present paper makes reference to a further insight into the geo-structural features and the litho-stratigraphic set-up of the Fontana Monte slope, as illustrated in Fig. 2 and Fig. 3. Indeed, the combination of newly available stratigraphies of continuous coring borehole (SC2, SC3 and S1V) and data resulting from large to detailed scale (Cascini, 2008) geo-structural survey have made possible the definition of a new geological and geomorphological map presented in Fig. 2. According to this map, the old town of Volturino lies on the calcareous member of the Faeto Flysch (recalled as FAEc herein), which is in contact with the TPC formation, outcropping to the west, and with the clayey member of the Faeto Flysch formation (recalled as FAEa), outcropping to the east, as shown by the sections in Fig. 3.

The longitudinal section of the slope, Section 1 in Fig. 3a, crosses the landslide body and extends further beyond the Giardino stream along the direction of the watershed, in order to set a distance between the vertical downslope side of the model and the toe of the landslide body. Within this section, the outcropping TPC formation overlies the FAEc member, which in turn is underlain by the clayey member of the Faeto Flysch (FAEa). At depth, the Red Flysch (FYR) overthrusts the Sub-Apennine Blue Clays (ASub). The two members FAEa and FAEc have been distinguished in the sections as resulting from the geological analyses, comprehensive of new field data and stratigraphic profiles.

The analysis of the inclinometric monitoring data reveals the presence of an active shear band at about 24 m depth in borehole SD1, located in the rear scarp of the landslide body, whereas along inclinometer SD2, within the landslide body, the occurrence of a shear band has been recorded between 45 and 55 m (confirmed by the presence of remoulded clay between 43.5 m and 45 m depth) and the inclinometric measurements along S1V borehole, in the rear scarp, are indicative of a

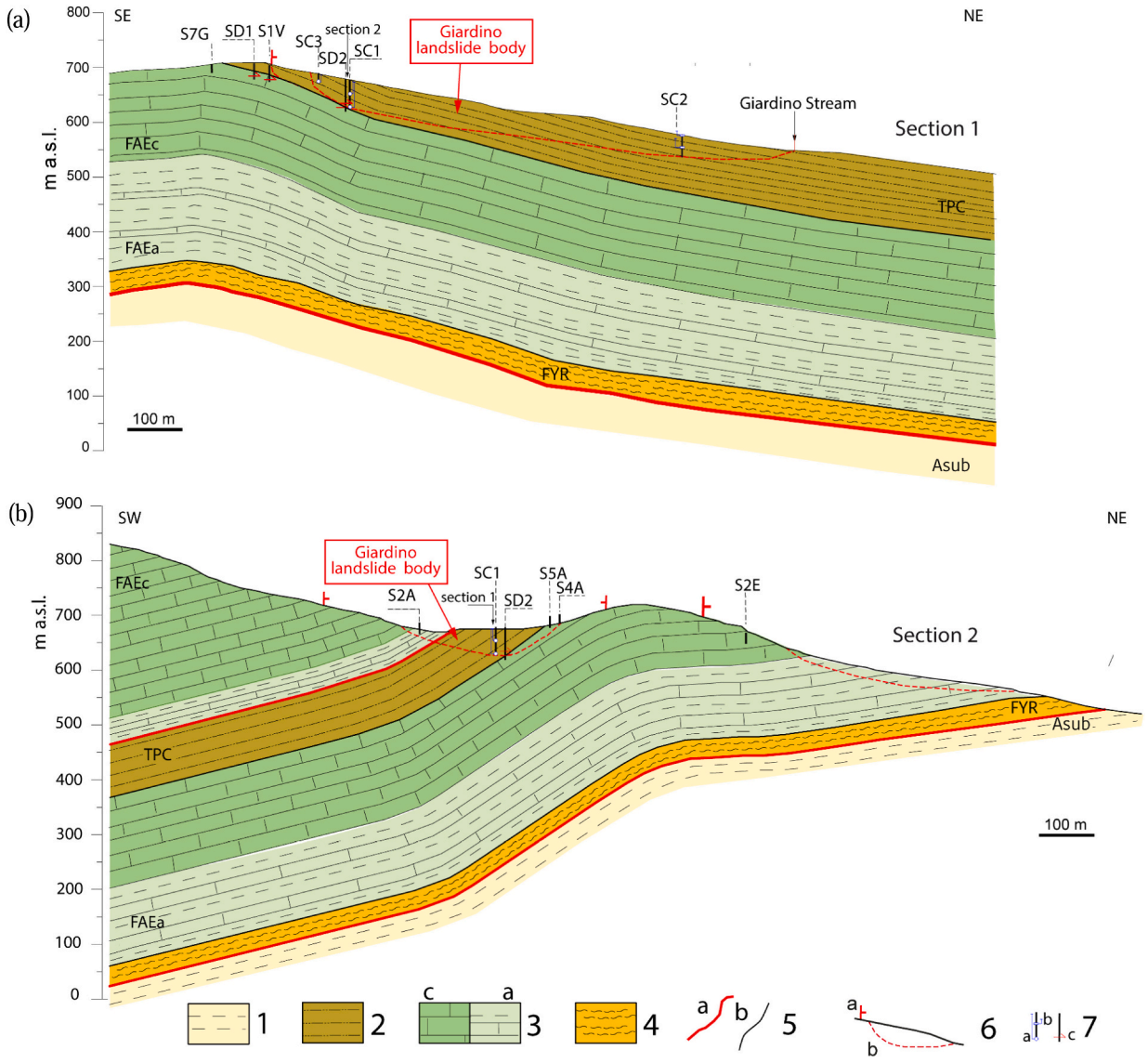

Fig. 3. Geological sections: (a) longitudinal Section 1 and (b) cross Section 2 (trace in Fig. 2). Legend: 1. Asub; 2. TPC; 3. Limestone member (FAEc) (c) and clayey member (FAEa) (a) of Faeto Flysch; 4. FYR; 5. Overthrust (a) and stratigraphic contact (b); 6. Landslide (a-crown, b-body); 7. Boreholes hosting piezometer (a-Casagrande cell, b-electric cell) and inclinometers with shear bending (c).

shear band at 27 m below ground surface. Based on all these evidences, the sliding surface of the landslide body has been defined along Section 1, as shown in Fig. 3a. Accordingly, the investigation data have been of reference in the design of the prototype slope modelling discussed in the following.

3. Numerical modelling of the SLVA interaction

3.1. The prototype slope model

Uncoupled two-dimensional H analyses of the transient seepage in a slope model have been carried out using the finite element software Seep/w (*Geo-Slope International*, 2004), making reference to the longitudinal Section 1 (Fig. 3a). A mesh discretization with 6-noded triangular elements has been employed for the whole domain, while a more refined mesh, with elements of about 0.2 m, has been adopted close to the ground surface, where time dependent boundary conditions are applied (Fig. 5). As recognised through the up-to-date stratigraphic analysis (e.g. data from SC2, SC3 and S1V), a 6 m thick layer of fractured clay (fractured topsoil), overlaying the marly TPC clay layer and both the FAEc and FAEa strata, has been implemented in the FE model along the whole section, accounting for partial saturation during part of the year. Furthermore, the FAEc has been set to outcrop at the top of the model.

The coefficient of saturated permeability k_{sat} of the TPC clay has been evaluated to be about 10^{-11} m/s based upon oedometer tests, while in-situ measurements, performed by means of variable-head tests in the SC1 piezometers, have detected a value of 10^{-9} m/s (Lollino et al., 2016). This is in accordance with typical observations for slopes made of fissured clays, for which the slope-scale saturated permeability is higher than that measured in the laboratory of even two orders of magnitude (Cotecchia et al., 2014). Moreover, the saturated permeabilities of FAEc and FAEa have been found to be about $5{\cdot}10^{-6}$ m/s and $5{\cdot}10^{-8}$ m/s, respectively, through water infiltration tests performed with the Guelph pressure infiltrometer (Lollino and Godt 2010, personal communication; Mazzei, 2010). Due to the lack of information about the hydraulic properties of the fractured topsoil, two values for the saturated permeability have been assumed and the corresponding hydraulic slope response has been investigated.

The hydraulic response of the partially saturated soils above the

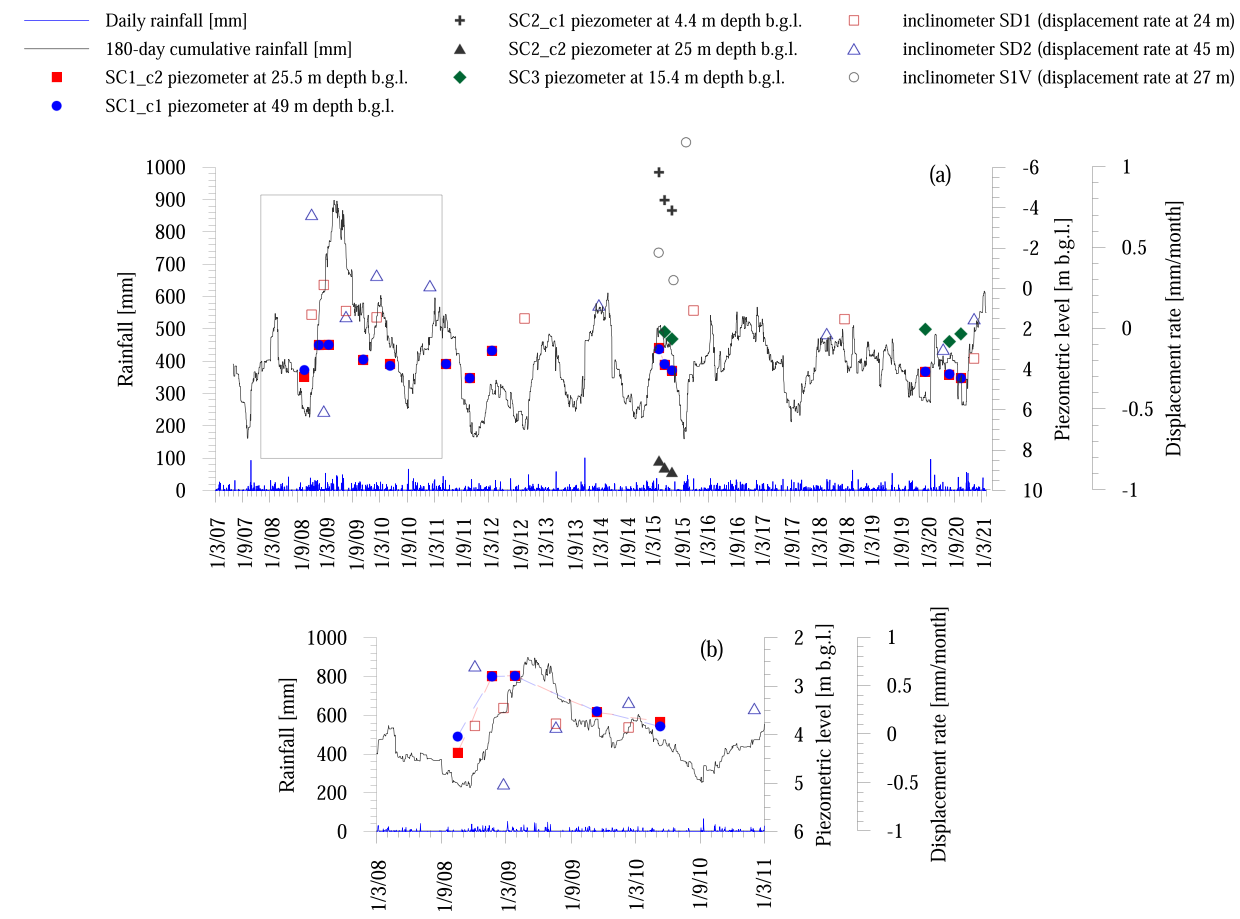

Fig. 4. Recorded rainfalls and in-situ monitoring data (a) over the period from 2008 to 2021 and (b) over the period from 2008 and 2011 (i.e. piezometric levels and displacement rates - Inclinometric and piezometric data from 2008 till 2013 are reported in Lollino et al., 2010 and 2016, while new measurements were conducted from 2015 to 2021).

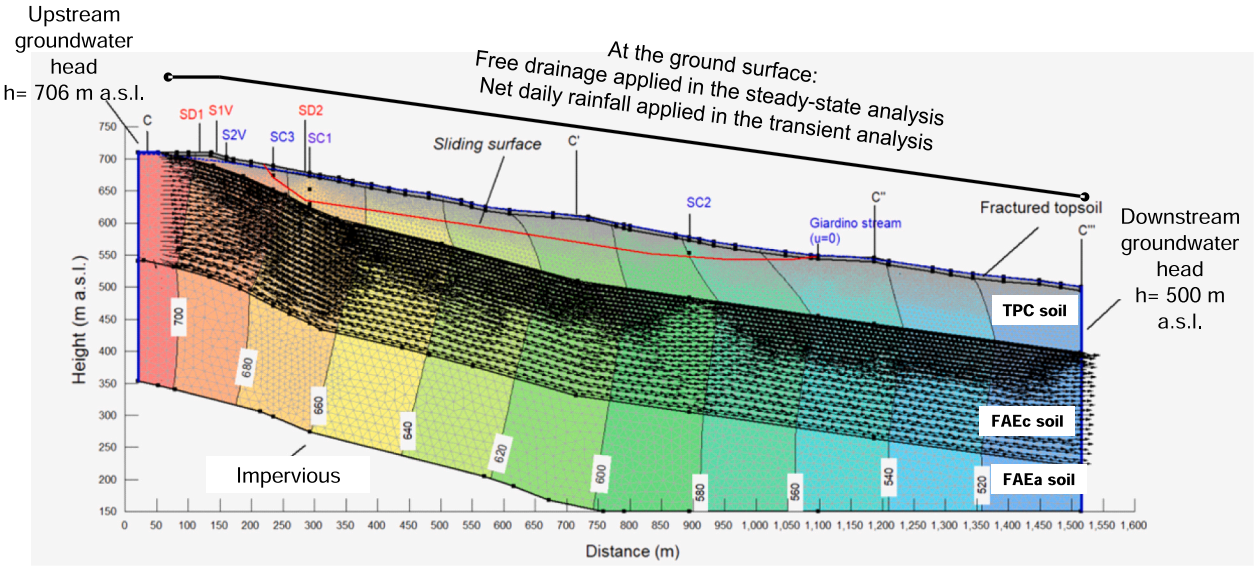

Fig. 5. FE slope model, boundary conditions, equipotential lines and flow velocity vector obtained at the end of the steady-state simulation under summer condition.

water table has been simulated through the hydraulic conductivity function and the water retention curve (WRC), $\theta_w = n \cdot S_r$ (where θ_w is the volumetric water content and S_r the degree of saturation). The WRCs, modelled according to van Genuchten (1980), using the parameters *a*, *m* and *n*, have been calibrated for each soil layer based on literature data available for the geomaterials tested in the same geo-hydro-mechanical context of reference (Fig. 6a). Due to the absence of direct experimental data, the retentive properties of the TPC clay have been considered very

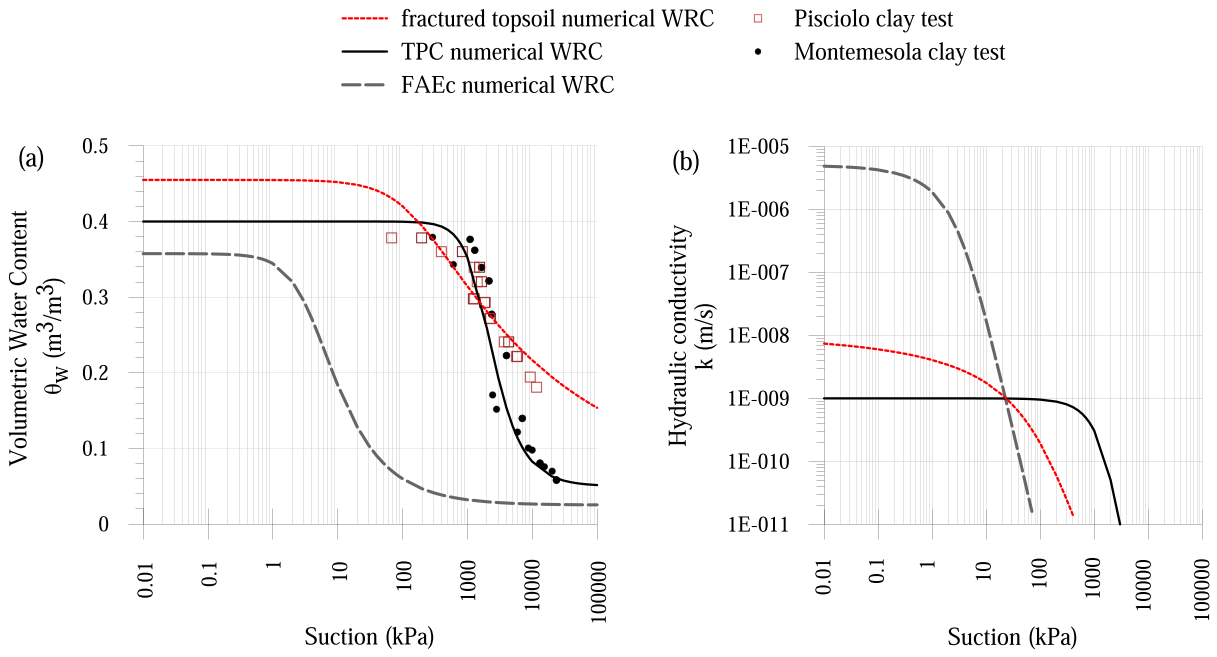

Fig. 6. (a) Numerically implemented water retention curves compared to laboratory test data, i.e. Pisciolo and Montemesola clay tests and (b) hydraulic conductivity function adopted in the FE model.

close to those of the Montemesola clay (Cafaro and Cotecchia, 2015; black symbols in Fig. 6a), which may be considered an upper boundary of the WRC of the class of clays, which the TPC clay belongs to. In particular, the WRC of fissured clays has been found to be controlled by the intact clay elements between the fissures (Cotecchia et al., 2014; Pedone, 2014; Tagarelli and Cotecchia, 2020a). Therefore, the stiff Montemesola clay has been considered similar to the intact TPC clay. The fractured topsoil, characterised by a clayey portion with sandy interlayers, has been modelled adopting typical retention curves measured through drying-wetting laboratory tests on clayey debris covering the slopes in the GHM context of reference (red symbols in Fig. 6a), as reported by Cotecchia et al. (2019a) and Tagarelli and Cotecchia (2020a). The WRC typical of medium-grained soils (Bottiglieri et al., 2012) has been assumed to be representative of the hydraulic behaviour of the heterogeneous and fractured calcareous portion of the Faeto Flysch. The hydraulic conductivity functions, shown in Fig. 6b, have been simulated according to the Mualem's assumption (Mualem, 1976).

In saturated conditions, the soil deformability is implemented through the volumetric compressibility coefficient under oedometric conditions, m_v, which is strictly related to the gradient of the WRC for positive pore water pressures. This value should be small enough to prevent soil straining at depth in the slope, since the effects of the hydro-mechanical coupling is not simulated (Elia et al., 2017). According to the observation that stiffness increases with depth, the compressibility coefficient has been assumed equal to 10^{-7} 1/kPa for the deeper soil layers, while a parametric analysis has been carried out to evaluate the effect of the fractured topsoil compressibility coefficient on the slope piezometric response. A summary of the hydraulic and retentive parameters adopted in the hydraulic FE simulations is reported in Table 1, where θ_{sat} and θ_{res} are the saturated and residual volumetric water content, respectively, while a, n and m are the fitting parameters of the Van Genuchten model.

The hydraulic boundary conditions of the model (Fig. 5) have been set accounting for the three-dimensional hydrogeological set-up of the hillslope, derived from the cited geological and hydrogeological surveys of the area. Accordingly, the calcareous portion of FAEc outcropping upstream is deemed to be location of a constant water table, feeding the underground seepage, along with the water coming from the upstream underground boundary. The latter has been assumed to be location of

Table 1
Hydraulic and retention parameters adopted in the FE simulations for the WRC and permeability functions.

Soil layer	θ_{sat} (%)	θ_{res} (%)	a (kPa)	n	m	k_{sat} (m/s)	m_v (1/kPa)
Fractured topsoil	45.5	5	135.7	1.21	0.171	variable	Variable
TPC soil	40	5	1694.9	2.33	0.572	1.00E-09	Variable
FAEa soil	40	5	1694.9	2.33	0.572	5.00E-08	1.00E-07
FAEc soil	35.75	2.5	3.8	1.69	0.408	5.00E-06	1.00E-07

hydrostatic condition, with constant water table (w.t.) at 4 m below ground level (b.g.l.). This assumption is realistic, when modelling the very low-rate steady-state seepage through the much lower permeability clays of the slope. Given the presence of the Giardino stream in the middle portion of the slope, the w.t. has been set at the ground surface (i.e. pore pressure equal to zero) where the section intersects the stream. Also, the downstream underground boundary has been set to be hydrostatic, with a w.t. at the ground surface, coherently with the proximity of the slope section to the watershed represented by the Giardino stream. The bottom boundary of the model has been assumed impervious, consistently with the low permeability of the deep clays. During the initial summer-like steady-state analysis, free drainage has been imposed to the top boundary of the FE model, in order to estimate the initial pore water pressure distribution, whose corresponding equipotential lines are shown in Fig. 5. The results of the summer-like steady-state simulation have been achieved adopting a saturated permeability k_{sat} equal to 10^{-8} m/s for the fractured topsoil, while the compressibility coefficient m_v assigned to the fractured topsoil and the TPC soil layers has been equal to 10^{-7} 1/kPa. The water table, resulting from the permanent seepage analysis performed employing such boundary conditions, is located close to the ground surface, according to the field observations in the slope. In addition, the quite good agreement between the numerical results and the average summer-like piezometric level, not shown herein for the sake of brevity, validates the selected hydraulic boundary conditions.

The results of the steady-state seepage analysis allow to identify the FAEc layer as a high piezometric head - bearing stratum, underlying the much less permeable TPC layer. The seepage rates are much higher within the FAEc (see the black flow velocity vectors in Fig. 5) than in the TPC clays, which are location of high piezometric heads at large depth, just close to the slip surface. Therefore, the new permanent seepage analyses demonstrate that the FAEc aquifer represents the source of the high piezometric heads at large depths in the clays.

Once the initial hydraulic conditions have been simulated, the transient seepage analysis has been performed imposing, at the top boundary, the climatic boundary condition rehearsed by the net daily rainfall of the year 2013–2014 (Fig. 7), which has been simulated for 12 years. As the transient simulations have been performed on a daily basis, the total duration of the analyses has been of 4377 days. The total daily rainfalls and temperatures measured at the Volturino weather station are shown in Fig. 7a and b.

The 2013–2014 thermo-pluviometric year has been chosen as representative of the average climatic conditions within the GHM context of reference over a long time period. The selection of this representative year has been carried out based on the analysis of the climate over the thirty-year period 1980–2010, defined as "near climate" by climatologists. As illustrated in Fig. 8, showing the total 180-day cumulative rainfalls from 1980 to 2010, together with the average 180-day cumulative rainfall over the 30 years, the average pluviometric year is characterised by a rainy period during winter, alternating a dry one during summer. The 180-day cumulative rainfall for the year 2013–2014 presents higher values during winter and small cumulative values during September–December and June–August periods, with an increase between December and June.

The net daily rainfall (Fig. 7d) has been evaluated as the difference between the total daily rainfall and the evapotranspiration flux (Fig. 7c), the latter estimated following the dual crop coefficient approach of the FAO Penman-Monteith method (Allen et al., 1998) through Eq. (1):

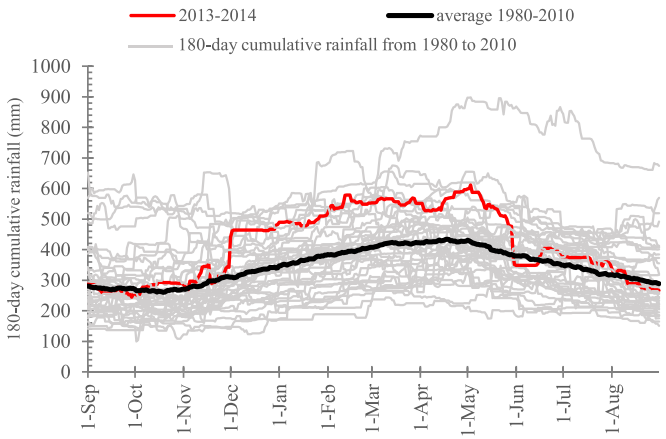

Fig. 8. 180-day cumulative rainfall over 30 years, from 1980 to 2010, together with the average 180-day cumulative rainfalls over the same period and the 180-day cumulative rainfall for the selected year 2013–2014.

$$ET_{c,adj} = E_{c,adj} + T_{c,adj} = K_e ET_0 + K_s K_{cb} ET_0 \quad (1)$$

where ET_0 is the reference evapotranspiration, K_e is the soil evaporation coefficient, which applies to the non-vegetated ground surface of the slope, K_{cb} is the basal crop coefficient, depending on the type and growth of the vegetation during the year, K_s is the water stress coefficient, which considers the effect of water stress on the crop transpiration. The evapotranspiration fluxes have been evaluated on a daily basis, assuming the presence of the winter wheat as plant type, covering the 70% of the slope throughout the year, as observed in-situ. The basal crop coefficient values K_{cb} assumed for each growth period, expressed in days, are summarised in Table 2, while the single components of transpiration $T_{c,adj}$, evaporation $E_{c,adj}$ and evapotranspiration $ET_{c,adj}$ fluxes

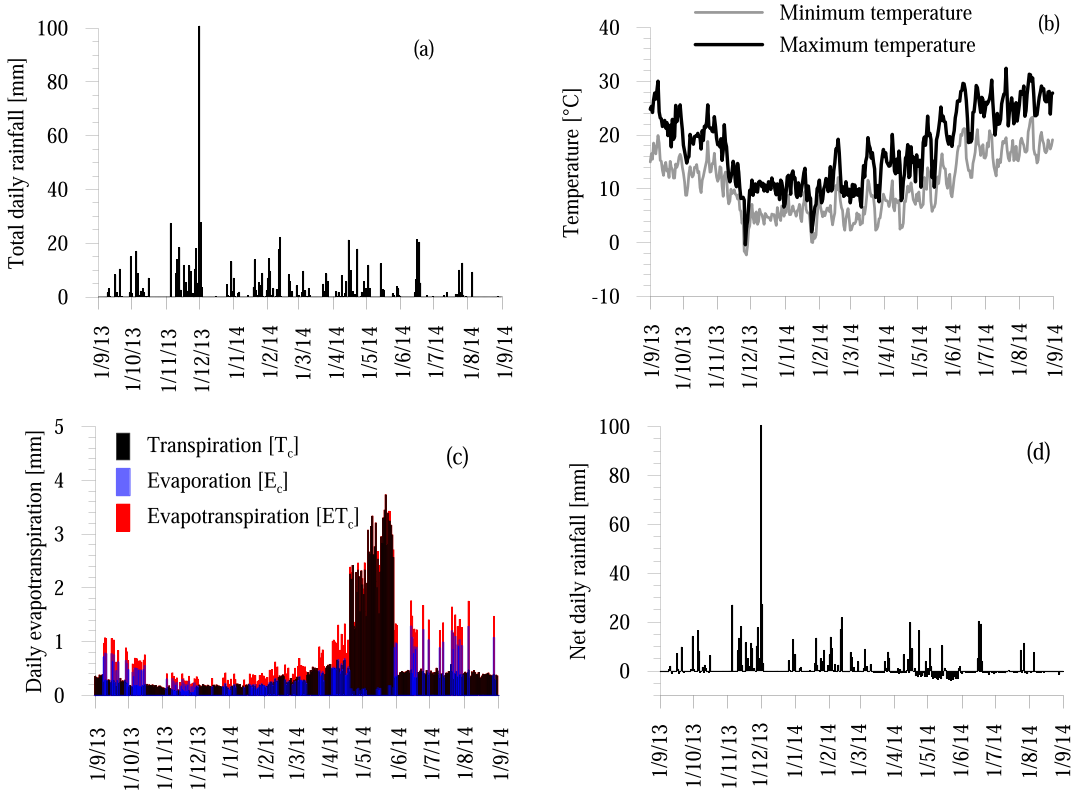

Fig. 7. Representative thermo-pluviometric year 2013–2014 adopted in transient FE modelling as top boundary condition: (a) Total daily rainfall, (b) minimum and maximum temperature, (c) daily evapotranspiration (d) net daily rainfall.

Table 2
Basal crop coefficient for winter wheat vegetation averaged cultivated over 70% soil portion.

Vegetation growth stage	Initial stage	Crop development	Mid-season	Late season
Period of the year(days)	1st Nov–30th Nov (30 days)	1st Dec–19th Apr (140 days)	20th Apr–29th May (40 days)	30th May–28th Jun (30 days)
K_{cb}	0.15	0.4	1.05	0.15

are reported in Fig. 7c. It is evident that the maximum evapotranspiration from the ground surface is achieved between the end of April and the end of June.

Following the procedure suggested by Tagarelli and Cotecchia (2020a), a simple root-water uptake model has been implemented in the analysis by applying the total rainfall at the ground surface, the negative evaporation flux at 0.05 m depth and the negative transpiration flux at 0.25 m depth b.g.l. The results of the seepage analysis are discussed in the following and compared with the monitoring data along SC1 (see Figs. 2–4), at 25.5 m and 49 m depth.

3.2. *Effects of the permeability of the fractured topsoil*

It is known that the hydraulic properties of the shallower soil layers and their change during the year control the water infiltration and evapotranspiration at the top boundary of a slope. Thus, the influence of the saturated permeability coefficient assigned to the fractured topsoil layer on the piezometric response of the Fontana Monte slope has been investigated.

To this aim, a first set of transient seepage analyses has been performed assuming two different values for the saturated permeability of the fractured topsoil, i.e. $1{\cdot}10^{-7}$ and $1{\cdot}10^{-8}$ m/s, respectively two order and one order of magnitude higher than that of the underlying TPC. The predicted variation of pressure heads with time at 25.5 m and 49 m depth along the borehole SC1 is shown in Fig. 9, together with the comparison with the monitored piezometric data.

Irrespective of the hydraulic properties of the fractured topsoil layer, the seasonal piezometric head fluctuations are more significant at small depth, i.e. at 25.5 m, where a variation of about 3 m is predicted between the end of summer and the end of winter, compared to fluctuations of no more than 1.5 m monitored in situ (see Fig. 9a). A less significant piezometric excursion is predicted in the deeper level, i.e. at 49 m depth, of about 0.5 m, in contrast with the much higher in-situ measurements (see Fig. 9b). Hence, the numerical results confirm that, even at a considerable depth, e.g. 25 m, the piezometric regime in the slope is still influenced by the climatic action along the sloping boundary of the system, where the rest of the boundary conditions have been set as steady. Conversely, the numerical predictions suggest that the source of the monitored high piezometric oscillations at 49 m depth should be sought in either other boundary processes, or other slope factors.

The pattern followed by the piezometric fluctuations is strongly influenced by the saturated permeability of the shallow layer. When a value of $1{\cdot}10^{-7}$ m/s is adopted, the pressure head rapidly increases at the end of summer, reaching its maximum value and oscillating around it until the beginning of the next summer, when it reduces to the

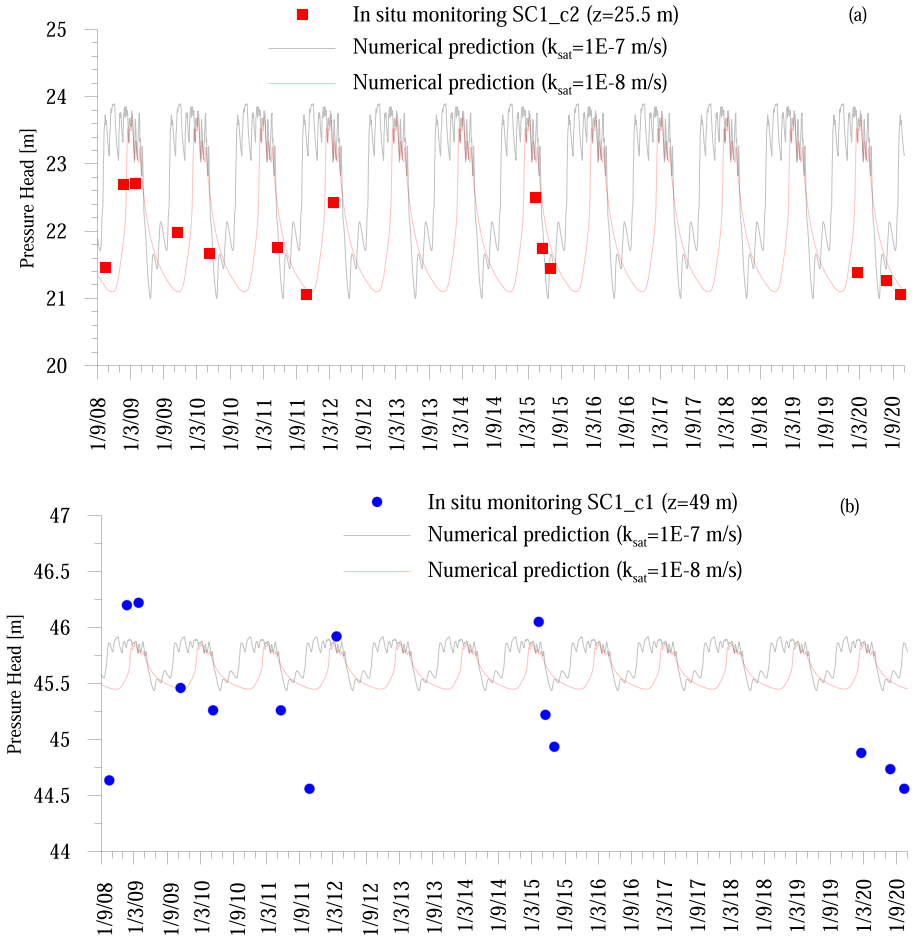

Fig. 9. Effect of the saturated permeability of the top fractured soil: numerical predictions compared to monitoring piezometric data at (a) 25.5 m and (b) 49 m depth.

minimum value. This is likely to be due to a rapid water infiltration process, not counteracted by the evapotranspiration fluxes, which promotes the accumulation of water stored in the slope with time. This behaviour tends to be mitigated when a less permeable soil with $k_{sat} = 1{\cdot}10^{-8}$ m/s is considered. In this case, the pressure head reaches its minimum value at around mid-autumn, when it starts to increase up to the maximum, achieved at the end of winter, before decreasing again in summer. Such hydraulic response reflects on the pattern followed by the factor of safety varying with time, as it modifies the amplitude of the critical period of landslide activity. This is an important issue to be dealt with, since it has an impact on the periods during which particular attention should be paid for the occurrence of landslide accelerations on the slope, especially in the context of early warning systems.

3.3. Effects of the compressibility coefficient m_v

It has been already recognised that the compressibility coefficient m_v affects the hydraulic numerical prediction of the slope model (Cotecchia et al., 2014). In uncoupled analyses, the selection of this value should be guided by the necessity of preventing volumetric soil straining at depth in the slope (Elia et al., 2017; Cotecchia et al., 2019a). To such aim, the above-described analyses have been carried out assuming a homogenous value of the compressibility coefficient, equal to $1{\cdot}10^{-7}$ 1/kPa for all the soil strata.

In order to evaluate the impact of this soil parameter on the pore water pressure distribution in the slope, further simulations have been performed, varying the m_v value assigned to the fractured topsoil and the TPC soil layers and adopting a saturated permeability of 10^{-8} m/s for the topsoil. The first simulation has been carried out assuming m_v equal to $5{\cdot}10^{-5}$ 1/kPa for both soil layers, as deduced from oedometer tests, while the second simulation accounts for the increase in stiffness with depth assigning a value of m_v equal to $5{\cdot}10^{-5}$ 1/kPa to the topsoil and $1{\cdot}10^{-7}$ 1/kPa to the TPC layer (named "combined m_v" analysis in Fig. 10).

The numerical results of this set of analyses, together with the previous results obtained assuming a homogeneous m_v equal to 10^{-7} 1/kPa, are presented in Fig. 10a in terms of pressure head variations with time at 25.5 m depth for only 2 years. As expected, the use of the higher compressibility coefficient, i.e. $5{\cdot}10^{-5}$ 1/kPa, generates an extremely small oscillation of the piezometric level with time, as already recognised by Cotecchia et al. (2014). The combination of the two m_v values, instead, induces a pressure head fluctuation characterised by slightly lower peak values occurring at the end of March and a more regular pattern between March and May, if compared to the analysis with a homogeneous m_v equal to 10^{-7} 1/kPa. This tendency is confirmed when the hydraulic response at 49 m depth is observed (Fig. 10b).

3.4. Impact of the variability with time of the hydrogeological boundary conditions

With the purpose of investigating the causes that produce the significant piezometric excursions at large depths, additional transient seepage analyses have been conducted accounting for the seasonal variation of the hydrogeological boundary condition within the calcareous aquifer bounding the seepage in the TPC layer. Thus, the impact of the seasonal recharge of the aquifer present in FAEc have been simulated and its effect on the stability of the landslide body has been investigated in terms of FoS.

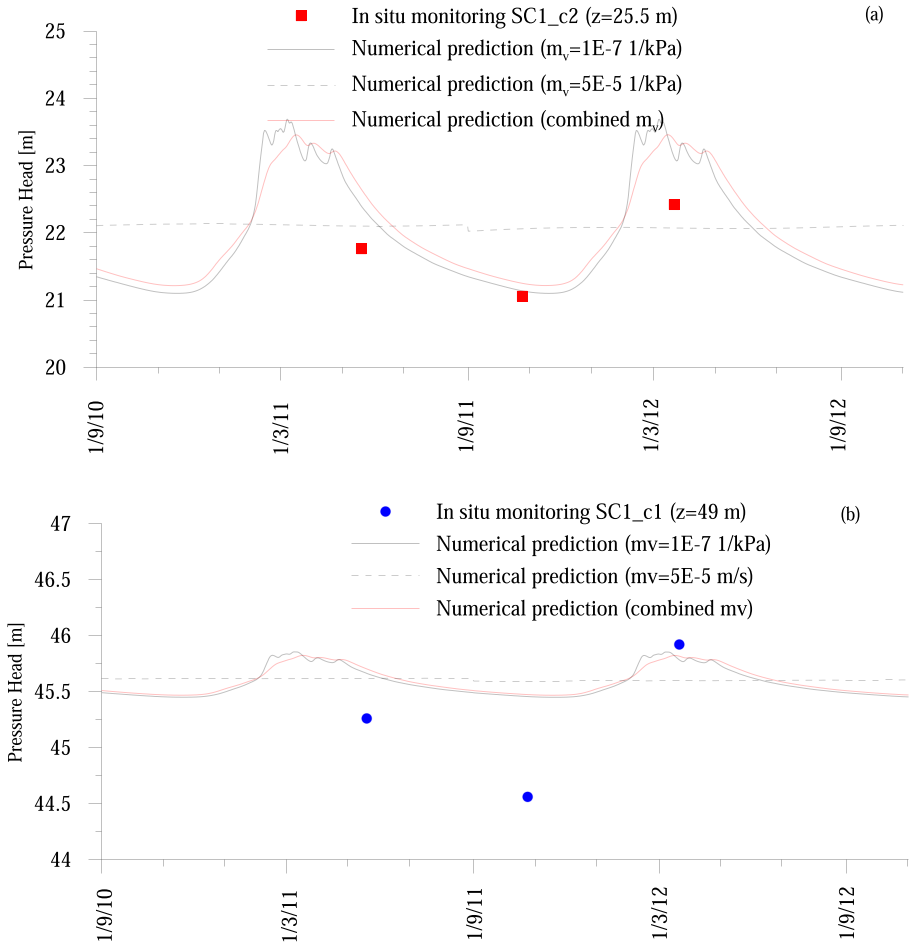

Fig. 10. Effect of the compressibility coefficient: numerical predictions compared to monitoring piezometric data at (a) 25.5 m depth and (b) 49 m depth.

The underground FAEc aquifer is fed in the upstream recharging area, as made evident by the presence of the Fontana Monte spring just about the contact between the less permeable FAEa unit with the more permeable FAEc portion (see Fig. 2). Thus, the accurate modelling of the seepage regime in the slope requires a proper simulation of the groundwater-level fluctuation in the aquifer, connected to the weather conditions over the year. Therefore, a simplified approach has been adopted to implement the effects of the groundwater recharge of the aquifer, which have been simulated as the variation with time of the aquifer water table, i.e. of the piezometric head along the upstream hydrostatic boundary condition.

Therefore, the upstream hydraulic boundary condition has been assumed to vary with time according to a sinusoidal function (Eq. (2)) characterised by a period T of 365 days, oscillating between the summer-like hydrostatic piezometric, h_{summer}, and winter-like, h_{winter}, groundwater heads:

$$h(t) = \left(\frac{h_{\text{summer}} + h_{\text{winter}}}{2}\right) - \left(\frac{h_{\text{winter}} - h_{\text{summer}}}{2}\right) sen\left(\frac{2\pi t}{T} + \frac{\pi}{2}\right) \quad (2)$$

The minimum head, h_{summer}, has been assumed to occur in late summer, i.e. the 1st of September, while the maximum head, h_{winter}, is reached in late winter, i.e. the 1st of March, in accordance with the general pattern of the 180-day cumulative rainfall typically observed in these regions. The first analysis has been performed considering an excursion of the groundwater head of 1 m between summer and winter, with a w.t. oscillating between 3 and 4 m b.g.l. The second hydraulic condition has been simulated by varying the upstream w.t. between 3.5 and 5 m b.g.l, this latter being a new initial summer-like steady-state condition. In these simulations, a saturated permeability of 10^{-8} m/s and a compressibility coefficient m_v of $5{\cdot}10^{-5}$ 1/kPa have been adopted for the fractured topsoil.

The numerical results, reported in Fig. 11, give evidence to the great impact of the seasonal excursion of the upstream boundary condition on the hydraulic response of the slope at large depth. Indeed, while the variation with time of the groundwater head only slightly affects the pressure head fluctuation at 25 m depth (see Fig. 11a), a far more significant excursion of the piezometric head occurs at 49 m depth, due to the aquifer recharge (see Fig. 11b). Furthermore, the analysis reveals that the hydraulic recharge determining a piezometric head oscillation between 3.5 m and 5 m determines variations of the piezometric heads in the clays closest to the monitored ones.

Therefore, the numerical simulations of the transient seepage reveal how the rainfall infiltration along the slope mainly affects the strata down to 25 m b.g.l., while at larger depths the piezometric fluctuation is largely related to the seasonal recharge of the deep aquifer. Furthermore, the new hydraulic modelling highlights that the presence of the deep calcareous aquifer in the slope is the source of the very high piezometric level measured about the base of the TPC clay layer through the piezometer at 49 m down SC1. Such level is very close to the piezometric level measured at 25.5 m down the same borehole. Hence,

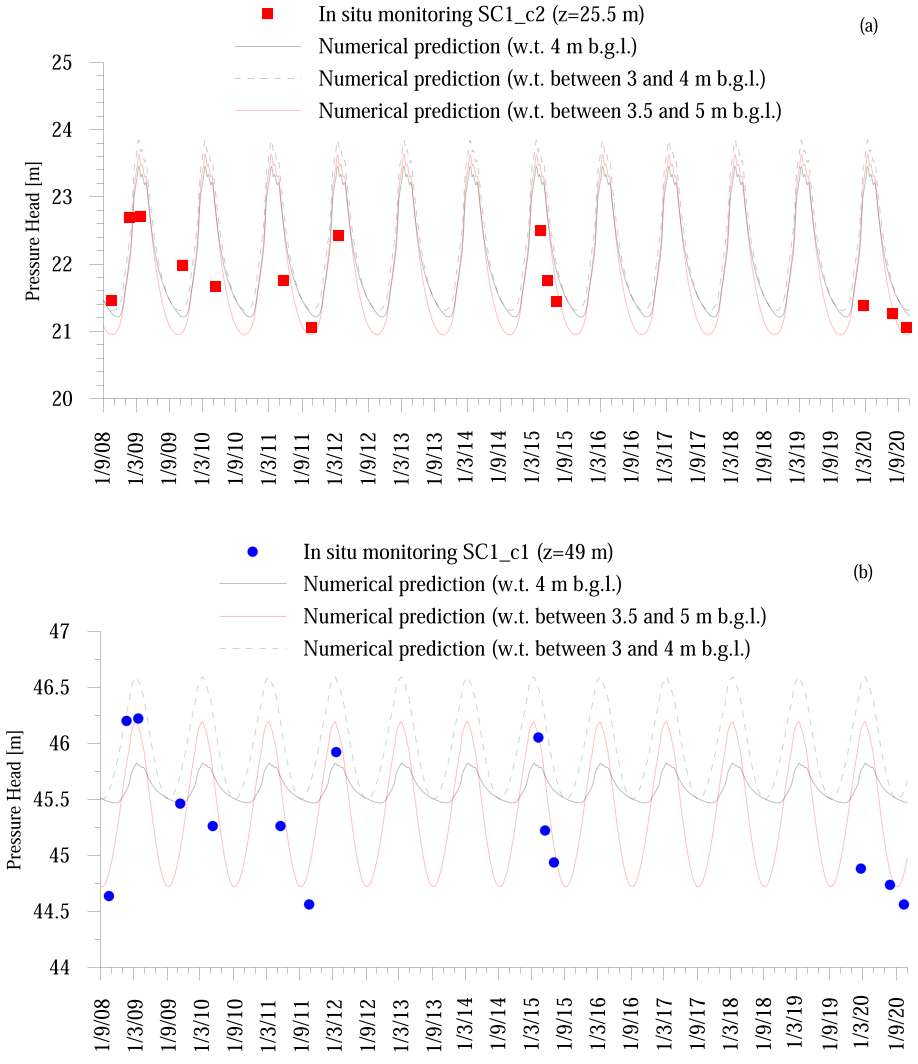

Fig. 11. Effect of the hydrogeological boundary condition: numerical predictions compared to monitoring piezometric data at (a) 25.5 m and (b) 49 m depth.

the simulations demonstrate how important for a correct prediction of the seepage regime is the thorough reconstruction of the geo-structural and hydrogeological set-up of the slope and of its surroundings, which are main ingredients of the slope model.

4. Slope stability analyses

In order to evaluate the impact of both the weather and the hydro-geological factors on the stability of the Fontana Monte landslide, LE analyses of the deep landslide body have been carried out implementing the pore water pressure distributions resulting from the transient seepage simulations.

The LE analyses have been undertaken using the Morgenstern and Price method, implemented in the software Slope/w (*Geo-Slope International,* 2004), which adopts the Mohr-Coulomb failure criterion modified to account for partial saturation (Fredlund and Rahardjo, 1993) as expressed by Eq. (3):

$$\tau_f = c' + \sigma_n tan(\varphi') + stan(\varphi_b') \quad (3)$$

where φ'_b is the friction angle accounting for the increase in shear strength due to suction s. Given that the degree of saturation S_r above the water table attains a minimum value at the ground surface, of about 80% during the dry season, and that the deep slip surface develops mainly in the saturated portion of the slope, it is reasonable to assume φ'_b equal to the mobilised friction angle φ'.

The variation of the factor of safety, FoS, during the year has been computed for the pre-imposed slip surface, about 900 m long, reconstructed through field geomorphological surveys, inclinometric data and stratigraphic records of weakened soil portions (Fig. 3 and Fig. 5). For such slip surface, assuming the summer-like steady-state hydraulic conditions (i.e. w.t. at 4 m b.g.l.) and a homogeneous unit weight of 18.8 kN/m^3, a mobilised effective friction angle φ'_m equal to 19.2° has been determined, which is just slightly lower than the peak φ'_p equal to about 20°, measured through laboratory tests for the TPC soil samples (Lollino et al., 2016, 2010).

Then, using the mobilised effective friction angle $\varphi'_m = 19.2°$, LE analyses have been undertaken implementing the pore water pressure distribution variable with time, resulting from the transient seepage analyses performed assuming at the upstream boundary either the constant water table at 4 m b.g.l. or the variable water table oscillating between 3.5 m and 5 m b.g.l. In this second analysis, since the initial summer-like permanent condition is simulated with constant water table at 5 m b.g.l., the initial safety factor $FoS_{initial}$ is greater than one. In order to make the LE results comparable, the variation with time of the current FoS normalised to the initial $FoS_{initial}$ (achieved under the initial steady-state summer-like conditions of each analysis) are represented for different upstream boundary conditions (Fig. 12). Normalised FoS results are illustrated with reference to three consecutive years, together with the time distribution of the associated pressure heads at 49 m depth (i.e. at SC1_c1 piezometer cell), close to the slip surface.

The pattern of the normalised FoS variation is characterised by a fluctuation between a minimum value in early spring and a maximum value in mid-autumn. Indeed, the FoS is subjected to an increase from the end of March to early November, concurring with the decrease of the pressure head, and it reduces from the second part of autumn to the end of winter, when the piezometric head increases, reaching its minimum value in mid-March, irrespective of the applied upstream boundary condition.

With respect to the analysis assuming a constant piezometric head upstream, the interaction of the TPC clay with the aquifer recharge provides a slight reduction of the maximum FoS attained during the dry season. The difference between the peaks obtained during the two simulations is equal to 1%. However, the accurate prediction of the piezometric head fluctuation, through the simulation of the interaction of the hydraulic recharge area with the atmosphere, impacts on the critical periods of landslide activity. Indeed, considering the FoS curve relative to the variable groundwater head analyses, the landslide body becomes unstable between February and May, and it recovers its stability at the beginning of summer. Nevertheless, the limit equilibrium results confirm the seasonal nature of the landslide reactivations, as they are in agreement with the monitored displacement rates and surveied structural damages. Indeed, the FoS oscillates between values of about 1.07÷1.08 in the dry season to values of 1 during the wet season, when the slope is marginally stable, with an overall variation of less than 10%.

5. Conclusions

The numerical investigation of the piezometric regime and stability conditions of the prototype slope, representing the GHM features of several slopes in the South-Eastern Apennines, confirms that very high piezometric heads may occur down to large depths, due to the contact of the slope soils, either at large depth or laterally, with water-bearing rocky aquifers of high permeability. Indeed, the low strength parameters of the clays in the slopes, together with the cited high piezometric heads represent factors, predispose the slope to instability in the GHM context of reference. Moreover, the presence of the underground

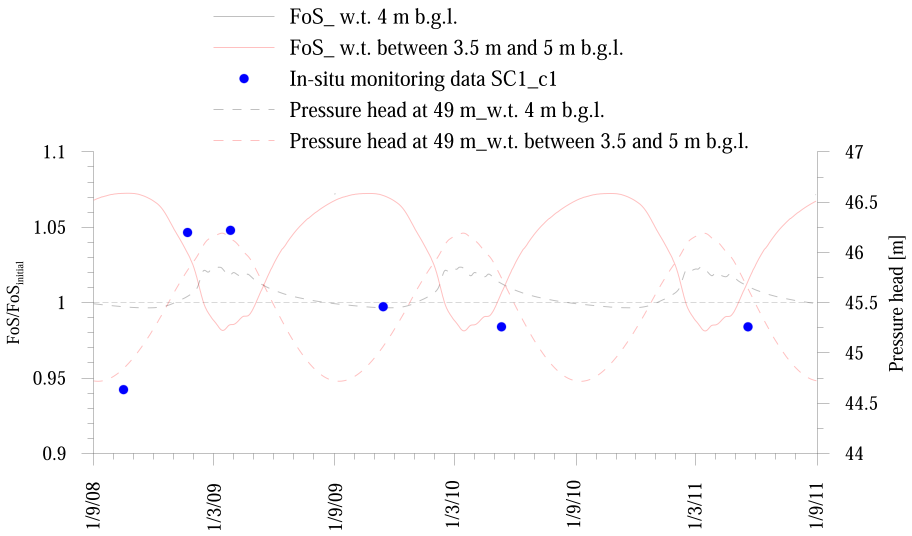

Fig. 12. Variation of the normalised FoS of the landslide body and pressure head at 49 m depth with time.

aquifer, fed by an upstream hydraulic recharging area, may be co-responsible of seasonal piezometric head fluctuations, due to the vegetation-atmosphere interaction over the whole hillslope. Therefore, the paper reports an advancement in the modelling of the SLVA interaction phenomena in the cited GHM context, as it highlights how these depend on the interaction with climatic actions not only of the soils at the slope top boundary, but also of the underground aquifers bordering the clay slope.

In particular, the SLVA interaction has been simulated by inputting a net flux at the sloping surface, accounting for the monitored rainfalls and the evapotranspiration, while the recharge of the deep aquifer during the year has been modelled using a sinusoidal function of the groundwater head. Considering these boundary conditions, the transient seepage modelling results show that the high piezometric heads measured at large depth in the slope clays are controlled by the hydrogeological regime of the hillslope, while their seasonal fluctuations are due to both the water infiltration along the sloping surface, connected to the weather conditions, and the groundwater recharge of the calcareous aquifer. Moreover, the input of such simulations into limit equilibrium analyses allows to predict realistic seasonal reactivations of the landsliding in the slope.

Funding

The research is funded by both the European Social Fund (ESF) through the National Operational Program Research and Innovation 2014–2020 “Attraction and International Mobility” (PON-AIM project code AIM1871082) and the Italian Ministry for Research and University “PRIN 2015” grant (Prot. 201572YTLA).

Declaration of Competing Interest

The authors declare that they have no known competing financial interests or personal relationships that could have appeared to influence the work reported in this paper.

Acknowledgments

The authors are grateful to the Southern Apennine District Basin Authority for providing in-situ data obtained in the context of the “Executive project for geognostic investigation and monitoring aimed at updating the knowledge about the hydrographic basin of the Candelaro stream for the municipalities of Alberona (FG), Castelluccio Valmaggiore (FG), Faeto (FG), Motta Montecorvino (FG) and Volturino (FG)”.

References

Allen, R.G., Pereira, L.S., Raes, D., Smith, M., 1998. Crop evapo-transpiration (guidelines for computing crop water requirements). In: FAO Irrigation and Drainage Paper No. 56. Rome, Italy.

Alonso, E.E., Gens, A., Delahaye, C.H., 2003. Influence of rainfall on the deformation and stability of a slope in overconsolidated clays: a case study. Hydrogeol. J. 11, 174–192. https://doi.org/10.1007/s10040-002-0245-1.

Bottiglieri, O., Cafaro, F., Cotecchia, F., 2012. Estimating the retention curve of a compacted soil through different testing and interpretation methods. In: Unsaturated Soils: Research and Applications. Springer Berlin Heidelberg, pp. 47–54. https://doi.org/10.1007/978-3-642-31116-1_7.

Brönnimann, C., Stähli, M., Schneider, P., Seward, L., Springman, S.M., 2013. Bedrock exfiltration as a triggering mechanism for shallow landslides. Water Resour. Res. 49, 5155–5167. https://doi.org/10.1002/WRCR.20386.

Cafaro, F., Cotecchia, F., 2015. Influence of the mechanical properties of consolidated clays on their water retention curve. Ital. Geotech. J. 49, 11–27.

Cafaro, F., Cotecchia, F., Santaloia, F., Vitone, C., Lollino, P., Mitaritonna, G., 2017. Landslide hazard assessment and judgment of reliability: a geomechanical approach. Bull. Eng. Geol. Environ. 76, 397–412. https://doi.org/10.1007/s10064-016-0966-3.

Cai, Z., Ofterdinger, U., 2016. Analysis of groundwater-level response to rainfall and estimation of annual recharge in fractured hard rock aquifers, NW Ireland. J. Hydrol. 535, 71–84. https://doi.org/10.1016/j.jhydrol.2016.01.066.

Calvello, M., Cascini, L., Sorbino, G., 2008. A numerical procedure for predicting rainfall-induced movements of active landslides along pre-existing slip surfaces. Int. J. Numer. Anal. Methods Geomech. 32, 327–351. https://doi.org/10.1002/nag.624.

Cascini, L., 2008. Applicability of landslide susceptibility and hazard zoning at different scales. Eng. Geol. 102, 164–177. https://doi.org/10.1016/j.enggeo.2008.03.016.

Cascini, L., Calvello, M., Grimaldi, G.M., 2010a. Groundwater modeling for the analysis of active slow-moving landslides. J. Geotech. Geoenviron. Eng. 136, 1220–1230. https://doi.org/10.1061/(asce)gt.1943-5606.0000323.

Cascini, L., Cuomo, S., Pastor, M., Sorbino, G., 2010b. Modeling of rainfall-induced shallow landslides of the flow-type. J. Geotech. Geoenviron. Eng. 136, 85–98. https://doi.org/10.1061/(asce)gt.1943-5606.0000182.

Cotecchia, F., Santaloia, F., Lollino, P., Vitone, C., Mitaritonna, G., 2010. Deterministic Landslide Hazard Assessment at Regional Scale, in: GeoFlorida 2010. American Society of Civil Engineers, Reston, VA, pp. 3130–3139. https://doi.org/10.1061/41095(365)319.

Cotecchia, F., Lollino, P., Mitaritonna, G., Elia, G., 2011. Interventi di stabilizzazione nei pendii nell’appennino dauno: analisi dello stato esistente e proposta di criteri innovativi. In: XXIV Convegno Nazionale Di Geotecnica. Naples, Italy, pp. 695–703.

Cotecchia, F., Pedone, G., Bottiglieri, O., Santaloia, F., Vitone, C., 2014. Slope-atmosphere interaction in a tectonized clayey slope: a case study. Ital. Geotech. J. 1, 34–61.

Cotecchia, F., Vitone, C., Santaloia, F., Pedone, G., Bottiglieri, O., 2015. Slope instability processes in intensely fissured clays: case histories in the Southern Apennines. Landslides 12, 877–893.

Cotecchia, F., Lollino, P., Petti, R., 2016a. Efficacy of drainage trenches to stabilise deep slow landslides in clay slopes. Geotech. Lett. 6, 1–6. https://doi.org/10.1680/jgele.15.00065.

Cotecchia, F., Santaloia, F., Lollino, P., Vitone, C., Pedone, G., Bottiglieri, O., 2016b. From a phenomenological to a geomechanical approach to landslide hazard analysis. Eur. J. Environ. Civ. Eng. 20, 1004–1031. https://doi.org/10.1080/19648189.2014.968744.

Cotecchia, F., Vitone, C., Petti, R., Soriano, I., Santaloia, F., Lollino, P., 2016c. Slow landslides in urbanised clayey slopes: An emblematic case from the south of Italy. In: Landslides and Engineered Slopes. Experience, Theory and Practice. Taylor and Francis Inc., pp. 691–698. https://doi.org/10.1201/b21520-79

Cotecchia, F., Tagarelli, V., Pedone, G., Ruggieri, G., Guglielmi, S., Santaloia, F., 2019a. Analysis of climate-driven processes in clayey slopes for early warning system design. Proc. Inst. Civ. Eng. - Geotech. Eng. 172, 465–480. https://doi.org/10.1680/jgeen.18.00217.

Cotecchia, F., Tagarelli, V., Vitone, C., Cafaro, F., Bottiglieri, O., Guglielmi, S., Santaloia, F., Lollino, P., 2019b. A geo-hydro-mechanical approach to landslide hazard assessment and mitigation: a successful application in Southern Italy. In: Global Assessment Report on Disaster Risk Reduction (GAR 2019).

Cotecchia, F., Santaloia, F., Tagarelli, V., 2020. Towards a geo-hydro-mechanical characterization of landslide classes: preliminary results. Appl. Sci. 10, 7960. https://doi.org/10.3390/app10227960.

Elia, G., Cotecchia, F., Pedone, G., Vaunat, J., Vardon, P.J., Pereira, C., Springman, S.M., Rouainia, M., Van Esch, J., Koda, E., Josifovski, J., Nocilla, A., Askarinejad, A., Stirling, R., Helm, P., Lollino, P., Osinski, P., 2017. Numerical modelling of slope–vegetation–atmosphere interaction: an overview. Q. J. Eng. Geol. Hydrogeol. 50, 249–270.

Elia, G., Falcone, G., Cotecchia, F., Rouainia, M., et al., 2020. Analysis of the effects of seasonal pore pressure variations on the slope stability through advanced numerical modelling. In: Geotechnical Research for Land Protection and Development. CNRIG 2019. Lecture Notes in Civil Engineering, vol. 40. Springer, doi:10.1007/978-3-030-21359-6.

Fredlund, D.G., Rahardjo, H., 1993. Soil Mechanics for Unsaturated Soils, Soil Mechanics for Unsaturated Soils. John Wiley & Sons, Inc., Hoboken, NJ, USA https://doi.org/10.1002/9780470172759.

Fredlund, D.G., Rahardjo, H., Fredlund, M.D., 2012. Unsaturated Soil Mechanics in Engineering Practice. New York.

Gens, A., 2010. Soil-environment interactions in geotechnical engineering. Geotechnique 60, 3–74. https://doi.org/10.1680/geot.9.P.109.

GeoStudio, User’s Guide, 2004. Geo-Slope International.

Greco, R., Comegna, L., Damiano, E., Guida, A., Olivares, L., Picarelli, L., 2014. Conceptual hydrological modeling of the soil-bedrock interface at the bottom of the pyroclastic cover of Cervinara (Italy). Procedia Earth Planet. Sci. 9, 122–131. https://doi.org/10.1016/J.PROEPS.2014.06.007.

Healy, R.W., Cook, P.G., 2002. Using groundwater levels to estimate recharge. Hydrogeol. J. 10, 91–109. https://doi.org/10.1007/s10040-001-0178-0.

Kenney, T.C., Lau, K.C., 1984. Temporal changes of groundwater pressure in a natural slope of nonfissured clay. Can. Geotech. J. 21, 138–146. https://doi.org/10.1139/t84-011.

Kovacevic, N., Potts, D.M., Vaughan, P.R., 2001. Progressive failure in clay embankments due to seasonal climate changes. Proceedings 5th International Conference on Soil Mechanics and Geotechnical Engineering, Istanbul 2127–2130.

Leroueil, S., 2001. Natural slopes and cuts: Movement and failure mechanisms. Geotechnique 51, 197–243. https://doi.org/10.1680/geot.2001.51.3.197.

Lollino, P., Elia, G., Cotecchia, F., Mitaritonna, G., 2010. Analysis of Landslide Reactivation Mechanisms in Daunia Clay Slopes by Means of Limit Equilibrium and FEM Methods. Geotechnical Special Publication, pp. 3155–3164. https://doi.org/10.1061/41095(365)322.

Lollino, P., Cotecchia, F., Elia, G., Mitaritonna, G., Santaloia, F., 2016. Interpretation of landslide mechanisms based on numerical modelling: two case-histories. Eur. J. Environ. Civ. Eng. 20, 1032–1053. https://doi.org/10.1080/19648189.2014.985851.

Lorenzo-Lacruz, J., Garcia, C., Morán-Tejeda, E., 2017. Groundwater level responses to precipitation variability in Mediterranean insular aquifers. J. Hydrol. 552, 516–531. https://doi.org/10.1016/j.jhydrol.2017.07.011.

Losacco, N., Bottiglieri, O., Santaloia, F., Vitone, C., Cotecchia, F., 2021. The geo-hydro-mechanical properties of a turbiditic formation as internal factors of slope failure processes. Geosciences 11, 429. https://doi.org/10.3390/GEOSCIENCES11100429.

Lu, N., Likos, W.J., 2004. Unsaturated Soil Mechanics | Wiley. Wiley, New York.

Mazzei, F., 2010. Analisi numerica della filtrazione in un pendio in frana ai fini di valutazioni della stabilità. MSc Thesis. Technical University of Bari, Bari, Italy.

Mualem, Y., 1976. A new model for predicting the hydraulic conductivity of unsaturated porous media. Water Resour. Res. 12, 513–522. https://doi.org/10.1029/WR012i003p00513.

Ng, C.W.W., Shi, Q., 1998. Influence of rainfall intensity and duration on slope stability in unsaturated soils. Q. J. Eng. Geol. 31, 105–113. https://doi.org/10.1144/GSL.QJEG.1998.031.P2.04.

Olivella, S., Carrera, J., Gens, A., Alonso, E.E., 1994. Nonisothermal multiphase flow of brine and gas through saline media. Transp. Porous Media 15, 271–293. https://doi.org/10.1007/BF00613282.

Olivella, S., Gens, A., Carrera, J., Alonso, E.E., 1996. Numerical formulation for a simulator (CODE_BRIGHT) for the coupled analysis of saline media. Eng. Comput. (Swansea, Wales) 13, 87–112. https://doi.org/10.1108/02644409610151575.

Palmisano, F., Vitone, C., Cotecchia, F., 2018. Assessment of Landslide damage to buildings at the Urban Scale. J. Perform. Constr. Facil. 32, 04018055. https://doi.org/10.1061/(asce)cf.1943-5509.0001201.

Pedone, G., 2014. Interpretation of Slow and Deep Landslides Triggered by Slope-Atmosphere Interac-Tion in Slopes Formed of Fissured Clayey Turbidites. Technical University of Bari, Bari, Italy.

Pedone, G., Ruggieri, G., Trizzino, R., 2018. Characterisation of climatic variables used to identify instability thresholds in clay slopes. Géotechnique Lett. 8, 231–239. https://doi.org/10.1680/jgele.18.00020.

Pedone, G., Tsiampousi, A., Cotecchia, F., Zdravkovic, L., 2021. Coupled hydro-mechanical modelling of soil-vegetation-atmosphere interaction in natural clay slopes. Can. Geotech. J. https://doi.org/10.1139/cgj-2020-0479 cgj-2020-0479.

Piccinini, L., Berti, M., Simoni, A., Bernardi, A.R., Ghirotti, M., Gargini, A., 2014. Slope stability and groundwater flow system in the area of Lizzano in Belvedere (Northern Apennines, Italy). Eng. Geol. 183, 276–289. https://doi.org/10.1016/J.ENGGEO.2014.09.002.

Pirone, M., Damiano, E., Picarelli, L., Olivares, L., Urciuoli, G., 2012. Groundwater-atmosphere interaction in unsaturated pyroclastic slopes at two sites in Italy. Ital. Geotech. J. 66, 29–49.

Postill, H., Helm, P.R., Dixon, N., Glendinning, S., Smethurst, J.A., Rouainia, M., Briggs, K.M., El-Hamalawi, A., Blake, A.P., 2021. Forecasting the long-term deterioration of a cut slope in high-plasticity clay using a numerical model. Eng. Geol. 280, 105912 https://doi.org/10.1016/j.enggeo.2020.105912.

Rahardjo, H., Rezaur, R.B., Leong, E.C., 2009. Mechanism of rainfall-induced slope failures in tropical regions. In: Picarelli, L., Tommasi, P., Urciuoli, G., Versace, P. (Eds.), Proceeding of the 1st International Workshop on Landslides (IWL), pp. 31–42. Naples, Italy.

Rajeev, P., Chan, D., Kodikara, J., 2012. Ground-atmosphere interaction modelling for long-term prediction of soil moisture and temperature. Can. Geotech. J. 49, 1059–1073. https://doi.org/10.1139/T2012-068.

Rouainia, M., Davies, O., O'Brien, T., Glendinning, S., 2009. Numerical modelling of climate effects on slope stability. Proc. Inst. Civ. Eng. - Eng. Sustain. 162, 81–89. https://doi.org/10.1680/ensu.2009.162.2.81.

Rouainia, M., Helm, P., Davies, O., Glendinning, S., 2020. Deterioration of an infrastructure cutting subjected to climate change. Acta Geotech. 15, 2997–3016. https://doi.org/10.1007/s11440-020-00965-1.

Sitarenios, P., Casini, F., Askarinejad, A., Springman, S., 2021. Hydro-mechanical analysis of a surficial landslide triggered by artificial rainfall: the Ruedlingen field experiment. Geotechnique 71, 96–109. https://doi.org/10.1680/jgeot.18.P.188.

Smethurst, J.A., Clarke, D., Powrie, W., 2012. Factors controlling the seasonal variation in soil water content and pore water pressures within a lightly vegetated clay slope. Geotechnique 62, 429–446. https://doi.org/10.1680/geot.10.P.097.

Tagarelli, V., Cotecchia, F., 2020a. The Effects of Slope Initialization on the Numerical Model predictions of the Slope-Vegetation-Atmosphere Interaction. Geosciences 10, 85. https://doi.org/10.3390/geosciences10020085.

Tagarelli, V., Cotecchia, F., 2020b. Deep movements in clayey slopes relating to climate: modeling for early warning system design. In: Lecture Notes in Civil Engineering. Springer, pp. 205–214. https://doi.org/10.1007/978-3-030-21359-6_22.

Terzaghi, K., 1950. Mechanism of landslides. In: Application of Geology to Engineering Practice. Geological Society of America, pp. 83–123. https://doi.org/10.1130/berkey.1950.83.

Tommasi, P., Boldini, D., Caldarini, G., Coli, N., 2013. Influence of infiltration on the periodic re-activation of slow movements in an overconsolidated clay slope. Can. Geotech. J. 50, 54–67. https://doi.org/10.1139/cgj-2012-0121.

Tsiampousi, A., Smith, P.G.C., Potts, D.M., 2017. Coupled consolidation in unsaturated soils: from a conceptual model to applications in boundary value problems. Comput. Geotech. 84, 256–277. https://doi.org/10.1016/j.compgeo.2016.10.008.

Van Esch, J., Sellmeijer, J., Stolle, D., 2013. Modeling transient groundwater flow and piping under dikes and dams. In: Taylor, Francis (Eds.), Proceedings, Third International Symposium on Computational Geomechanics. London.

van Genuchten, M.T., 1980. A closed-form equation for predicting the hydraulic conductivity of unsaturated soils. J. Soil Sci. Soc. Am. 44, 892–898.

Vassallo, R., Grimaldi, G.M., Di Maio, C., 2015. Pore water pressures induced by historical rain series in a clayey landslide: 3D modeling. Landslides 12, 731–744. https://doi.org/10.1007/s10346-014-0508-7.

Vaughan, P.R., 1994. Assumption, prediction and reality in geotechnical engineering. Géotechnique 44, 573–609. https://doi.org/10.1680/geot.1994.44.4.573.

Vitone, C., Cotecchia, F., 2011. The influence of intense fissuring on the mechanical behaviour of clays. Géotechnique 61, 1003–1018.

Wang, K., Xu, Z.M., Tian, L., Ren, Z., Yang, K., Tang, Y.J., Gao, H.Y., Luo, J.Y., 2019. Estimating the dynamics of the groundwater in vegetated slopes based on the monitoring of streams. Eng. Geol. 259, 105160 https://doi.org/10.1016/J.ENGGEO.2019.105160.